

## $\beta$ -Carotene encapsulation in a mannitol matrix as affected by divalent cations and phosphate anion

Sonia C. Sutter, María P. Buera<sup>\*,1</sup>, Beatriz E. Elizalde<sup>2</sup>

*Departamento de Industrias, Facultad Ciencias Exactas y Naturales, Universidad de Buenos Aires, 1428 Ciudad Universitaria, Buenos Aires, Argentina*

Received 8 March 2006; received in revised form 11 September 2006; accepted 15 September 2006  
Available online 23 September 2006

### Abstract

The effects of addition of divalent cations and phosphate buffer on the degree of  $\beta$ -carotene encapsulation in a mannitol matrix during freeze-drying were analyzed. The degradation rate of encapsulated  $\beta$ -carotene as a function of % RH and its relationship with the physical state of the matrix during storage at 25 °C was also studied. The presence of phosphate salts significantly delayed mannitol crystallization at a highly satisfactory degree during freeze-drying and, consequently, the degree of  $\beta$ -carotene encapsulation increased. This effect was maintained over quite long time during storage of the freeze-dried samples at 25 °C. Unavoidable local variations in water content during 3 years storage caused the decrease of  $T_g$  values and made the crystallization degree to increase. The divalent cations showed a synergistic effect and also modified the kinetics of  $\beta$ -carotene degradation during storage, increasing its stability. The mechanism of crystallization inhibition likely includes a change in hydrogen bond network or/and change in molecular mobility in the presence of divalent cations and phosphate anions. The degradation rate of  $\beta$ -carotene in a mannitol/ $\text{KH}_2\text{PO}_4$  matrix increased as increasing % RH until a value at which the samples collapsed (75% RH), and then the degradation rate decreased. Collapse phenomena may affect diffusion of oxygen from the surface to the inside of the matrix and increase retention of  $\beta$ -carotene. Surface color was not an appropriate indicator for  $\beta$ -carotene degradation, because it was mostly dependent on the optical properties of the matrix, which changed with the degree of matrix hydration and collapse.

© 2006 Elsevier B.V. All rights reserved.

**Keywords:** Mannitol crystallization; Amorphous-state; Encapsulation;  $\beta$ -Carotene; Storage stability; Crystallization inhibitor

### 1. Introduction

$\beta$ -Carotene theoretically possesses 50% Vitamin A activity (Delgado Vargas et al., 2000) and its demand has increased due to its reported anticancer (Giovannucci, 1999; Nishino et al., 1999), free radical quencher and other biological antioxidant activities (Bendich and Olson, 1989; Murakoshi et al., 1999). The high degree of unsaturation in  $\beta$ -carotene structure renders it extremely susceptible to oxygen. Stability and retention of labile biomolecules during drying and the later storage are often dependent on their encapsulation in an amorphous matrix formed during dehydration processes (Tant and Wilkes, 1981; Roos and Karel, 1991; Maa et al., 1997, 1998a,b; Constantino

et al., 1998; Brazel, 1999; Qui and Xu, 1999; Pyne et al., 2003; Rodríguez-Huezo et al., 2004). Amorphous sugars are effective encapsulating agents. However, amorphous materials undergo a structural change at the glass transition temperature ( $T_g$ ), that affect the stability of encapsulated compound (Roos, 1987). Sugar crystallization as a consequence of storage above the glass transition temperature ( $T_g$ ), promotes both the release of encapsulated lipids (Shimada et al., 1991; Labrousse et al., 1992) and the loss of the stabilizing effect on biomolecules such as enzymes (Suzuki et al., 1997). The changes in the physical structure of matrix may also lead to increased permeability and diffusivity of gases ( $\text{H}_2\text{O}$ ,  $\text{O}_2$ ) that affect reaction rates and decrease stability of encapsulated active materials (Karel, 1991; Karel and Saguy, 1991; Maa et al., 1997).

Elizalde et al. (2002) showed that the magnitude of color change, the rate of  $\beta$ -carotene loss and the minimum retention of  $\beta$ -carotene encapsulated in a matrix of trehalose were mainly affected by the excess of moisture, above that necessary for trehalose dihydrate crystallization.

\* Corresponding author. Fax: +54 11 4576 3366.

E-mail address: [pilar@di.fcen.uba.ar](mailto:pilar@di.fcen.uba.ar) (M.P. Buera).

<sup>1</sup> Member of Consejo Nacional de Investigaciones Científicas y Técnicas de la República Argentina (CONICET).

<sup>2</sup> Researcher of Universidad de Buenos Aires.

In non-crystalline polymeric matrices the release of encapsulated material has been qualitatively related to structural collapse or shrinkage as a result of storage above the glass transition temperature ( $T_g$ ) of the matrix (Omatete and Judson King, 1978; Levi and Karel, 1995; Selim et al., 2000; Serris and Biliaderis, 2001). However, Prado et al. (2006) demonstrated that  $\beta$ -carotene losses were mainly observed in the glassy state (below  $T_g$ ), where the high porosity matrix allowed oxygen diffusion and then a fast  $\beta$ -carotene degradation. Oppositely, the lower degradation rate constants were observed under conditions at which the matrix was fully plasticized and the structural collapse caused the disappearance or the dramatic decreased of micropores of matrix.

Mannitol is a popular excipient used in freeze-dried formulations to stabilize biomolecules (proteins, enzymes, hormones, vitamins). Mannitol crystallization profiles, including those of its various polymorphs, have been studied extensively (Martini et al., 1997; Kim et al., 1998; Yu et al., 1999; Burger et al., 2000; Kett et al., 2003). Amorphous mannitol possesses some physical and functional properties different from those of crystallized solids (Pikal et al., 1991; Izutsu et al., 1993, 1994; Crowe et al., 1998; Johnson et al., 1991; Nail et al., 2002). For example, amorphous-state mannitol protects protein conformation during freeze-drying through hetero-solute molecular interaction with proteins (e.g. hydrogen bonding). Chemical stability at extreme pH conditions may provide the amorphous mannitol some advantages among various polyols and saccharides (Telang et al., 2003). Several approaches have been taken to produce amorphous-state containing solids. Obtaining amorphous pure mannitol by rapid cooling of a hot melt solution or freeze-drying aqueous mannitol solution are possible, but not practical because mannitol is physically unstable and will transform into a more stable crystalline form, even under ambient conditions (Telang et al., 2003; Yoshinari et al., 2003). Another and more practical approach is the freeze-drying for rapid cooling of mannitol and other amorphous component combinations (Pyne et al., 2002; Telang et al., 2003). Molecular level mixing with other components may limit spatial rearrangement of the mannitol molecules required for crystallization. In fact, various solutes that remain amorphous in frozen solutions and during freeze-drying (NaCl, POHK<sub>2</sub>, glycine) were reported to inhibit mannitol crystallization (Pikal et al., 1991; Izutsu et al., 1993, 1994; Randolph, 1997; Kim et al., 1998; Constantino et al., 1998; Fakes et al., 2000; Cavatur et al., 2002; Izutsu and Kojima, 2002; Pyne et al., 2003; Telang et al., 2003).

Altering molecular mobility in the amorphous phase by complex formation and/or molecular interaction is another approach to prevent mannitol crystallization. For example, the addition of a small amount of boric acid to hot melt mannitol solution retards crystallization from the amorphous solid (Yoshinari et al., 2003). Similarly, Izutsu et al. (2004) demonstrated that sodium tetraborate inhibit mannitol crystallization in frozen solution and freeze-dried solids by complexation.

It has been shown that the addition of divalent cations and transition metals enhanced the stabilizing effect of sugars and polyols on proteins (Carpenter et al., 1986, 1987a,b) and that

the addition of divalent cations delays trehalose crystallization (Mazzobze and Buera, 1999).

The objective of this work was to study the effects of divalent cations and phosphate anion on the degree of  $\beta$ -carotene encapsulation during freeze-drying, and on the kinetics of surface discoloration and of  $\beta$ -carotene degradation of in a mannitol matrix during storage at ambient conditions.

## 2. Materials and methods

### 2.1. Materials

Mannitol was from Merk Química Argentina S.A.I.C. (Buenos Aires, Argentina),  $\beta$ -carotene was obtained from Eurovit NS 30% (Warner Jenkinson Europe Ltd.), Gelatin (250 Bloom) was from Sanofi Bio-Industrias (Argentina S.A). All other chemicals were of analytical grade and purchased from Mallinckrodt Chemical Works (St. Louis, MO, USA).

### 2.2. Encapsulation method

0.2 g of a suspension of  $\beta$ -carotene (30%, w/v) was added to 350 mL of 15% mannitol solution in water or in K<sub>2</sub>HPO<sub>4</sub> buffer pH 7.4, prepared in a gelatin solution (0.15%, w/w), with and without addition of divalent cations salts (Table 1). Gelatin was previously dissolved in boiling water and was added as emulsifier (Shimada et al., 1991). Suspensions were agitated with an omni mixer at 16,000 rpm for 2 min twice. The approximate size of the emulsion oil droplets was 6–15  $\mu$ m, as determined semi-quantitatively by optical microscopy using a calibrated ocular micrometer.

The mixture was distributed in thin layers (about 10 mm) into Petri dishes and frozen at  $-26^\circ\text{C}$  for 24 h to obtain ice crystals with an adequate size to give a homogeneous, porous powder and then was immersed in liquid nitrogen ( $-190^\circ\text{C}$ ) before freeze-drying to allow the highest amount of freezable water to crystallize. An Heto-Holten A/S, cooling trap model CT 110 freeze-dryer (Heto Lab Equipment, Denmark) which operated at temperature of the condenser plate of  $-110^\circ\text{C}$  and at a minimum chamber pressure of  $4 \times 10^{-4}$  mbar. The main drying was performed without shelf temperature control and the chamber pressure ranged from 0.1 to below 0.01 mbar, which corresponds to ice temperatures from  $-45$  to below  $-60^\circ\text{C}$ , respectively. The temperature of the secondary dry-

Table 1  
Composition of solutions used to form matrices for  $\beta$ -carotene encapsulation

Formulation	Additive	Buffer
A	–	–
B	–	50 mM K <sub>2</sub> HPO <sub>4</sub> pH 7.4
C	–	10 mM K <sub>2</sub> HPO <sub>4</sub> pH 7.4
D	CaCl <sub>2</sub> ·2H <sub>2</sub> O 20 mM	10 mM K <sub>2</sub> HPO <sub>4</sub> pH 7.4
E	MgCl <sub>2</sub> ·6H <sub>2</sub> O 20 mM	10 mM K <sub>2</sub> HPO <sub>4</sub> pH 7.4
F	MnCl <sub>2</sub> ·4H <sub>2</sub> O 20 mM	10 mM K <sub>2</sub> HPO <sub>4</sub> pH 7.4
G	ZnCl <sub>2</sub> 20 mM	10 mM K <sub>2</sub> HPO <sub>4</sub> pH 7.4
H	Glycine 4 mM	–

All formulations contained 15% of mannitol.

ing was 25 °C, and the whole process lasted 48 h. The dried emulsions were broken and homogenized into powder by use of a mortar and pestle and subsequently washed with hexane (HPLC grade) to remove non-encapsulated surface carotene until negligible absorbance was detected at 452 nm. The washed powder was further dehydrated under vacuum over MgClO<sub>4</sub>. It was verified that during the homogenization of the freeze-dried samples no appreciated losses of encapsulated β-carotene had occurred.

### 2.3. Storage study

Aliquots of about 0.4 g of the dried samples were distributed into glass vials (3 mL capacity) and exposed to atmospheres of saturated salt solutions of 11% RH (LiCl), 44% RH (K<sub>2</sub>CO<sub>3</sub>) and 75% RH (NaCl) into evacuated desiccators at 25 °C (Greenspan, 1977). At selected times samples were removed and analyzed for water content, surface and encapsulated carotene, color and thermal transitions. All determinations were performed in triplicate and the average value was reported.

### 2.4. Determination of water content

The water content of the equilibrated samples was determined by difference in weight before and after drying into vacuum ovens at 98 °C during 48 h. These conditions had been proved to be adequate to assess constant weight after drying.

### 2.5. Thermal transitions

A differential scanning calorimetry (DSC) system (Mettler TA 4000 with a TC11 TA processor and Graph Ware TA72 thermal analysis software) was used for the thermal analysis. The instrument was calibrated using indium, zinc and lead. Analysis in duplicate involved aluminum pans (Mettler), 40 μL capacity hermetically sealed containing samples (between 5 and 10 mg). An empty pan was used as a reference.

Each sample was heated at a rate of 10 °C/min from –20 up to 170 °C (dynamic method) in order to determine glass transitions temperatures ( $T_g$ ), melting points ( $T_m$ ) and heats of fusion ( $\Delta H_m$ ) of mannitol in the formulations. Glass transitions were recorded as the onset temperature of the discontinuities in the curves of heat-flow versus temperature while the  $T_m$  value was taken to be the onset of melting peak.

The crystalline fraction of mannitol present in different formulations was calculated from the ratio of the area of the endothermic peak of mannitol in the sample and the calorimetric enthalpy of the melt of pure mannitol measured in the same conditions in dynamic DSC run:

$$\text{crystalline fraction} = \frac{\Delta H_s}{\Delta H_o}$$

where  $\Delta H_s$  is the heat of melting of mannitol in the formulations and  $\Delta H_o$  is the heat of melting of pure crystalline mannitol.

All the samples were prepared from the same freeze-dried batch and presented about 5% variability in the crystalline fraction among different samples.

### 2.6. Surface and encapsulated β-carotene

The procedures for determining surface and encapsulated β-carotene are based in the fact that β-carotene is lipophilic, and then soluble in hexane, being the matrix (mannitol) water soluble and insoluble in hexane. Surface carotene was determined by washing aliquots of ca. 0.08 g of the samples with 2 mL of hexane in a test tube and shook in a vortex for 2 min. This treatment was enough to remove all the surface carotene present. The powder was separated of hexane by decantation and the concentration of carotene in the hexane phase was measured spectrophotometrically at 452 nm. This wavelength was found to correspond to the maximum absorbance of the spectrum from 200 to 600 nm, and is in agreement with previous results reported by Lamikanra (1985), Chen (1992) and Desobry et al. (1997).

Encapsulated carotene was determined by dispersing the remaining powder with 1 mL of water and shaking in a vortex for 2 min (to dissolve the encapsulating mannitol matrix to liberate the encapsulated carotene). Then 2 mL of hexane were added and the suspension was shook for 2 min. The absorbance of the yellow to orange hexane fraction was measured at 452 nm, and expressed as absorbance units per gram of dry solids (a.u./g). The spectroscopic measurements were performed with a UV–vis spectrophotometer (UV-1203 Shimadzu).

The encapsulation degree (ED) during freeze-drying was calculated for each formulation as the μg of β-carotene obtained from the absorbance units of the hexane extracts (after dissolving the mannitol matrix in water), using the reported absorption coefficient for β-carotene per gram of dry solids (Szpylka and DeVries, 2005).

The percent of retention of encapsulated β-carotene (% R) was determined by dividing the ED at any time by the initial ED.

### 2.7. Surface color

A spectrophotometer Minolta 508-d (Minolta Co. Ltd., Tokyo, Japan) with integrating sphere was used to measure the chromatic characteristics of samples during storage. A standard calibration with white and black references was performed. To perform the measurements, samples were placed in a circular cell of 2 cm diameter. Calculations were done for Illuminant D65 (corresponding to the sun light distribution spectrum) and an observer angle (determined by the visual field and the horizon line) of 2°. X, Y and Z tristimulus values of the chromatic CIE (Commission Internationale de l'Eclairage) space were obtained. The chromatic coordinates  $L^*$ ,  $a^*$  and  $b^*$  (of the chromatic space CIE  $L^*a^*b^*$ ) were calculated through the following equations:

$$L^* = 116(Y/Y_n)^{1/3} - 16,$$

$$a^* = 500[(X/X_n)^{1/3} - (Y/Y_n)^{1/3}],$$

$$b^* = 200[(Y/Y_n)^{1/3} - (Z/Z_n)^{1/3}]$$

The  $L^*a^*b^*$  color space is an international standard for color measurement developed by CIE in 1976, which is the most often used in food research (37). The color definition in the  $L^*a^*b^*$

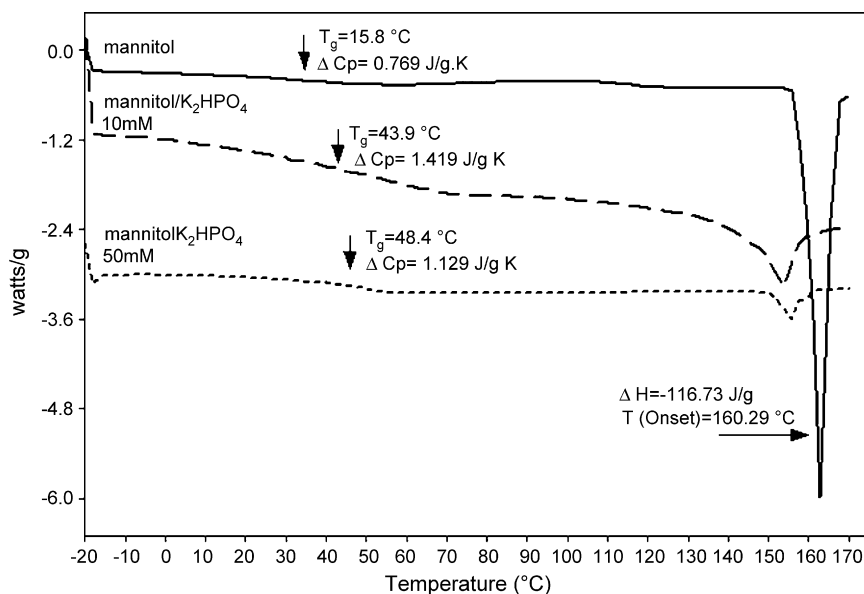


Fig. 1. DSC thermograms of mannitol samples A–C after freeze-drying, showing glass transitions and melting endothermals.

space consists of a luminance or lightness component ( $L^*$  value, ranging from 0 to 100), along with two chromatic components: the  $a^*$  component has positive values for red and negative values for green colors and the  $b^*$  component has positive values for yellow and negative values for blue colors.

### 2.8. Data analysis

The kinetic constants for carotene retention and surface color changes were obtained applying a non-linear regression analysis to the experimental data (Graph Pad Prism Version 3.1 Software). The corresponding standard deviations and the correlation coefficients between experimental values and those calculated through the model ( $R^2$ ) were obtained. All parameters were determined with 95% confidence intervals. The mathematical models employed to describe the experimental behavior are further detailed in the following section.

## 3. Results

### 3.1. Effect of buffer phosphate, divalent cations and glycine on the initial degree of encapsulation and surface color

Fig. 1 shows the DSC thermograms obtained for the freeze-dried samples with and without salts. As shown in Fig. 1, no mannitol crystallization was observed during heating the samples in the DSC runs. Thus, % crystallinity could be calculated based on the observed heat of melting, as detailed in Section 2. In control samples without buffer nor salt addition mannitol had crystallized at a high extent during the freeze-drying process and presented a pronounced endothermal peak corresponding to melting of crystalline mannitol (Fig. 1), at temperatures ( $T_m$ ) values from 155 to 160 °C. These  $T_m$  values were in accord with previous results (Yoshinari et al., 2003; Izutsu et al., 2004). These samples presented an almost 40% crystalline fraction and a  $T_g$  value of 18 °C. It is known (Telang et al., 2003; Yoshinari et

al., 2003) that mannitol crystallizes almost 100% during freeze-drying when no crystallization inhibitors are added to the formulation. Thus, the occurrence of almost 60% amorphous mannitol in the samples without salts is attributed to the presence of gelatine, added to stabilize the oil-in-water emulsion. The dispersed hydrophobic material, even in a very low concentration, may also act affecting the crystallization patterns through hydrophobic interactions (Gejl-Hansen and Flink, 1977; Etzel and Judson King, 1980; Naesens and Tobback, 1984).

Table 2 shows the characteristics (encapsulation degree, water content, surface color,  $a^*$ ,  $T_g$  values and crystallinity) of the samples after freeze-drying. As shown in Table 2, for formulations containing  $K_2HPO_4$  buffer  $\beta$ -carotene ED ( $\mu\text{g/g}$  dry matter) was 40- or 80-fold (depending on phosphate buffer concentration) compared to the samples without phosphate buffer and this was attributed to mannitol crystallization. Parameter  $a^*$  (related to surface color), showed a similar behavior. The  $T_g$  values of these samples increased as increasing phosphate buffer concentration (Table 2).

As also shown in Table 2, the amount of crystalline degrees after freeze-drying of the mannitol samples were 38% for the formulations without phosphate and 2% and 7% for the samples containing  $K_2HPO_4$  buffer 10 and 50 mM, respectively (they remained mostly amorphous, as discussed before in relation to Fig. 1). It was observed that the degree of crystallinity of the freeze-dried samples showed a slight increase during the first year of storage and it was 95% for mannitol samples and 65% in samples containing 10 or 50 mM phosphate in the third year. However, the  $T_g$  values of the samples had decreased during storage, which caused mannitol crystallization. The decrease of  $T_g$  values can be attributed to water redistribution in the dry emulsions or to water sorption from the samples due to the failure of the desiccant agent to maintain an anhydrous atmosphere. It is to be noted, however, that even at these unfavorable conditions mannitol crystallization was delayed in phosphate containing samples.



Table 2

Initial degree of encapsulation,  $T_g$  and parameter  $a^*$  (related to reddish surface color) for a mannitol matrix with and without phosphate salts

Matrix	ED (u.a./g dry matter) <sup>a</sup>	$a_0^{*b}$	Water content (%) <sup>c</sup>	$T_g$ (°C) <sup>d</sup>	% Cryst <sup>e</sup>
Mannitol	0.14	0.20	0.15	18.3	38
Mannitol + buffer phosphate 10 mM	1.19	1.35	0.55	43.9	2
Mannitol + buffer phosphate 50 mM	0.59	3.59	1.73	48.4	7

<sup>a</sup> ED is the encapsulation degree, calculated as  $\mu\text{g}\beta\text{-carotene/g dry matter}$ .

<sup>b</sup>  $a^*$  is the color coordinate related to the reddish characteristics of the samples.

<sup>c</sup> Water content is expressed as g water/100 g solids.

<sup>d</sup>  $T_g$  is the glass transition temperature.

<sup>e</sup> % Cryst. is the degree of mannitol crystallization, calculated as the percent of the melting enthalpy of mannitol in the sample related to the melting enthalpy of pure mannitol.

The presence of divalent cations increased the degree of encapsulation related to the matrix containing only phosphate buffer and mannitol, being the magnitude of this effect depending on the nature of cation in the order Zn (formulation G) > Mg (formulation E) > Ca (formulation D) > Mn (formulation F) (Fig. 2). As the water content of all freeze-dried matrices was approximately similar, independently of the salt involved (data not shown), the differences on encapsulation degree could not be attributed to the plasticizing effect of water.

The presence of glycine (formulation H) also increased the degree of encapsulation compared to the matrix containing only mannitol (Fig. 2). As observed before (Prado et al., 2006), the surface color change (parameter  $a^*$ ) was not representative of  $\beta$ -carotene retention inside the matrices (Fig. 2), because it was mostly affected by the change in optical properties (opacity).

### 3.2. $\beta$ -Carotene retention during storage

Mannitol–phosphate matrices (from solutions prepared with phosphate buffer 50 mM pH 7.4) were considered suitable formulations to analyze the retention of  $\beta$ -carotene during storage at 25 °C at several relative humidities.

In all analyzed cases, the concentration of surface  $\beta$ -carotene determined spectrophotometrically in the hexane washings was

negligible. However, this did not mean that all  $\beta$ -carotene remained encapsulated, but that  $\beta$ -carotene could not be detected on the surface during storage due to its fast degradation. Only the remaining fraction of encapsulated  $\beta$ -carotene before and after the storage experiments was analyzed in this work.

As shown in Fig. 3a, the general shape of the curves for the samples at RH of 11% and 44% consisted of an initial phase of fast loss, followed by a phase of slow loss, approaching an almost constant value (or plateau). The samples stored at RH 11% showed a 70%  $\beta$ -carotene retention (% R) after 63 days of storage while in the samples at 44% RH  $\beta$ -carotene degradation was almost total. Samples stored at 75% RH showed a completely different kinetic behavior, the curves presented three phases of degradation. The first is a fast loss phase followed by a phase of constant retention value (or plateau) and finally, the retention of  $\beta$ -carotene decreased abruptly. These differences in kinetic behavior were attributed to the fact that the samples at 75% RH were structurally collapsed (sticky aspect).

The obtained curves shown in Fig. 3a, for 11% and 44% RH were fitted according to the following model:

$$\ln \frac{R - R_\infty}{R_0 - R_\infty} = -k_D t \quad (1)$$

where  $R_0$  and  $R$  are the percentages of  $\beta$ -carotene retention at zero time and time  $t$ , respectively,  $R_\infty$  the asymptotic value to which the retention approaches at very long time and  $k_D$  is the rate constant for  $\beta$ -carotene loss. This model agrees with a first-order kinetic equation for the fractional retention. Karel and Saguy (1991) and Karel (1991) generalized Eq. (1) for any property subjected to change as result of a phase transition. The values of the constants  $k_D$ ,  $R_\infty$ , the corresponding standard deviations  $\sigma_{k_D}$ ,  $\sigma_{R_\infty}$  and the correlation coefficients between experimental values and those calculated through the model ( $R^2$ ) are reported in Table 3. The values calculated through Eq. (1) (full lines in Fig. 3a) fitted the experimental data with correlation coefficients ( $R^2$ ) higher than 0.97 ( $p < 0.05$  in all cases).

As shown in Fig. 3a and Table 3, the kinetic rate constant of  $\beta$ -carotene degradation in mannitol– $\text{H}_2\text{KPO}_4$  matrix increased as increasing RH for the samples at 11% and 44% (glassy state), whereas the asymptotic value ( $R_\infty$ ) diminishes. In the collapsed samples (those at RH 75%)  $\beta$ -carotene retention was intermediate between those at 11% and 44% up to 50 days, then it decreased abruptly being very low after 70 days (Fig. 3a).

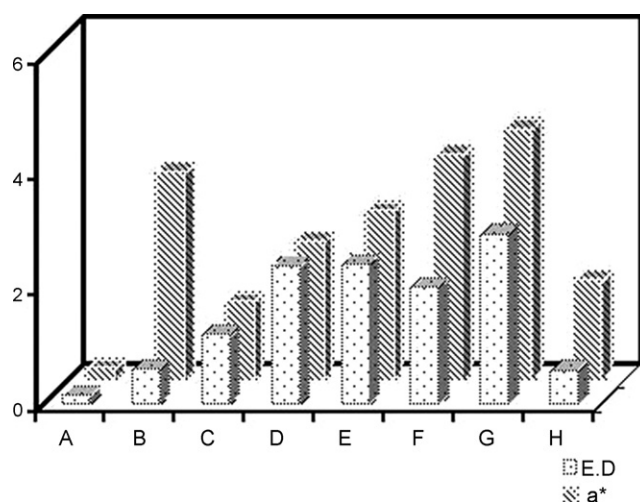
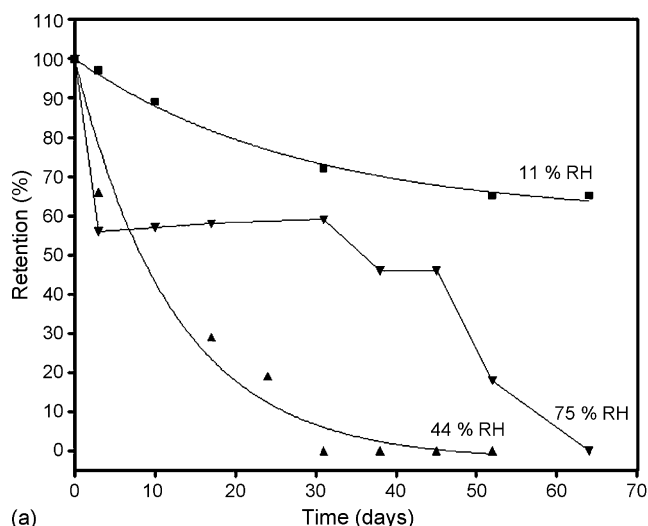
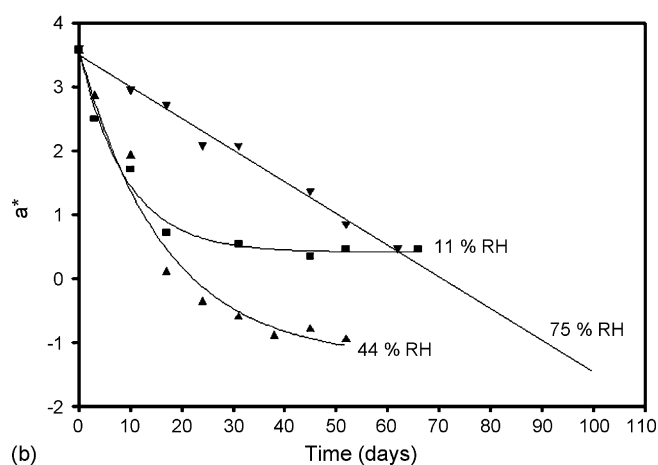


Fig. 2. Encapsulation degree (ED) in  $\mu\text{g}\beta\text{-carotene/g solids}$  and surface color (parameter  $a^*$ ) of  $\beta$ -carotene formulations after freeze-drying. A, B, C, D, E, F, G, H denote the system composition, as indicated in Table 1.



(a)



(b)

Fig. 3. (a) Percent of retention (% R) of  $\beta$ -carotene encapsulated in a mannitol matrix containing buffer phosphate 50 mM at pH 7.4 as a function of time, stored a 25 °C and at 11%, 44% and 75% of relative humidity (% RH). Symbols represent experimental data and solid lines predicted curves. (b) Variation of the colorimetric parameter  $a^*$  during storage of  $\beta$ -carotene encapsulated in a mannitol matrix (containing phosphate buffer 50 mM at pH 7.4) as a function of storage time at 25 °C and at 11%, 44% and 75% relative humidity (% RH). Symbols represent experimental data and solid lines predicted curves.

### 3.3. Surface color changes during storage

For a given formulation, a decrease of the red chromatic component ( $a^*$ ) of the sample surface was observed during storage.

The color function, luminosity  $L^*$  was very sensitive to the surface characteristics (glassy samples had very different sur-

Table 3

Kinetic rate constant values for  $\beta$ -carotene degradation in a mannitol matrix ( $k_D$ ), the asymptotic value ( $R_\infty$ ), the corresponding standard deviations ( $\sigma_{k_D}$ ), ( $\sigma_{R_\infty}$ ), respectively, and the correlation coefficients ( $R^2$ ) at different relative humidities (% RH) at 25 °C

RH (%)	Moisture content (%)	$k_D \pm \sigma_{k_D}$ (day <sup>-1</sup> )	$R_\infty \pm \sigma_{R_\infty}$	$R^2$
11	1.51	$0.035 \pm 0.005$	$60 \pm 3$	0.996
44	2.32	$0.081 \pm 0.01$	$2.20 \pm 1$	0.974
75*	7.02	–	–	–

\* Matrix collapsed.

face characteristics and diffusive/reflecting light properties from caked samples) and it was not representative of color changes. The chromatic coordinate  $b^*$  was neither a good indicator of  $\beta$ -carotene retention because it characterizes yellowness to blueness and these colors were not dominant. The chromatic coordinate  $a^*$  (redness), was found to be the more sensitive parameter to follow surface color changes. Fig. 3b shows the changes in redness ( $a^*$ ) as a function of storage time. It is to be noted that the negative values of  $a^*$  indicate a loss in redness. The curves presented an initial phase of rapid change and a later phase of slower change for samples at 11% and 44% of RH and were fitted according to the following equation:

$$\ln \frac{a^* - a_\infty^*}{a_0^* - a_\infty^*} = -k_{\text{color}} t \quad (2)$$

where  $a_0^*$  and  $a^*$  are the chromatic coordinates at zero time and time  $t$ , respectively;  $a_\infty^*$  the asymptotic value at the plateau and  $k_{\text{color}}$  is the first-order kinetic constant for color change.

Predicted color changes (full lines in Fig. 3b) showed good agreement with experimental points for the samples at 11% and 44% RH. The samples stored at RH 75% presented a different kinetic behavior. In fact, they presented a strong color compared to samples stored at 11% and 44% RH and followed at zero-order kinetic ( $a^* = 2.49 - 0.05t$ ,  $R^2 = 0.988$ ) (Fig. 3b). This different behavior can be attributed to the fact that the samples at 75% RH were collapsed and the matrix presented increased transparency.

The surface color values at the plateau ( $a_\infty^*$ ) increased with % RH while the kinetic constants ( $k_{\text{color}}$ ) were approximately independent on % RH (Table 4).

### 3.4. Effect of divalent cations and glycine on $\beta$ -carotene retention and surface color changes during storage

As showed in Section 3.1, the presence of divalent cations and glycine increased the initial degree of encapsulation and also changed the values of surface color, related to the matrix containing only phosphate buffer and mannitol, being the magnitude of this effect depending on the nature of the cation (Fig. 2). Then, it was considered interesting to study if this synergistic effect could be verify also on  $\beta$ -carotene retention and surface color changes during storage at different % RH

Table 5a shows the %  $\beta$ -carotene retention in mannitol matrices containing several divalent cations after 21 days of storage and at 11%, 44%, and 75% RH.

The magnitude of the effect was dependent of % RH and of nature divalent cation. In fact, at 11% RH the incorporation

Table 4

Kinetic rate constant values of surface color change ( $k_{\text{color}}$ ), parameter  $a^*$  value at infinite time ( $a_\infty^*$ ) with the corresponding standard deviations ( $\sigma$ ) and correlation coefficients ( $R^2$ ) between calculated and experimental values for  $\beta$ -carotene encapsulated in a mannitol matrix at different relative humidities (% RH) and at 25 °C

RH (%)	$(a_\infty^*) \pm \sigma_{(a_\infty^*)}$	$k_{\text{color}} \pm \sigma_{k_{\text{color}}}$ (day <sup>-1</sup> )	$R^2$
11	$0.412 \pm 0.08$	$0.111 \pm 0.012$	0.986
44	$-1.254 \pm 0.277$	$0.061 \pm 0.009$	0.978

Table 5a

Percentage of  $\beta$ -carotene retention encapsulated in a mannitol matrix in presence of different divalent cations or glycine after 21 days of storage at different relative humidities (RH) at 25 °C

Formulation	% Retention after 21 h		
	11% RH	44% RH	75% RH
C	44	21	26.4
D	44	23	52
F	97	15	12
G	100	33	28
H	40	42	35

of Zn (formulation G) and Mn (formulation F) to the 10 mM  $\text{KH}_2\text{PO}_4$ –mannitol (formulation C) increased  $\beta$ -carotene retention to approximately 100% compared to the matrix containing only phosphate (44% R). On the opposite, cation Ca (formulation D) had not any effect and the % of retention was similar to the matrix without Ca (Table 5a). At 44% and 75% RH no effect was found, except for Ca at 75% RH that increased the % of retention two-fold compared to the matrix containing only  $\text{KH}_2\text{PO}_4$ . The addition of glycine (formulation H) also increased almost two-fold  $\beta$ -carotene retention at all % RH.

The presence of divalent cations promoted also a change of surface color values related to the matrix containing only phosphate buffer and mannitol (Fig. 2).

Table 5b shows % of surface color loss after 21 h of storage calculated as  $((a_0^* - a_{21h}^*)/a_0^*) \times 100$ . At 11% RH all cations decreased approximately 50% surface color loss compared to the matrix without cations. At 44% the magnitude of reduction was in the order  $\text{Zn} > \text{Mn} > \text{Ca}$ . At 75% RH the transparency of matrices manitol–phosphate 10 mM (formulation D) and manitol–phosphate 10 mM + Ca (formulation E) increased during storage, and this was manifested on the negative values of surface color loss, as discussed in Section 3.3. On the other hand, the samples containing Mn (formulation F) or Zn (formulation G) remained opaque since these cations delayed structural changes and matrix collapse. At 11% RH a slight reduction on % of surface color loss was observed in glycine containing formulations whereas at 44% RH no effect of glycine was observed and at 75% RH the samples retained their structural appearance (not collapsed), as the formulations containing cations Zn and Mn.

Table 5b

Surface color loss after 21 h of storage of  $\beta$ -carotene encapsulated in a mannitol matrix in presence of different divalent cations or glycine at different relative humidities (RH) at 25 °C

Formulation	Surface color loss after 21 h of storage (%) <sup>a</sup>		
	11% RH	44% RH	75% RH
C	52	92.3	–75
D	20	66.6	–62
F	24.6	55.8	41
G	25	30	25
H	35	82	57

<sup>a</sup> % surface color loss after 21 h of storage calculated as  $((a_0^* - a_{21h}^*)/a_0^*) \times 100$ .

#### 4. Discussion

Mannitol crystallized at a great extent during freeze-drying and the presence of phosphate buffer diminished or inhibited the crystallization process. These results were in accord with those reported by Pikal et al. (1991), Izutsu et al. (1994), Randolph (1997), Izutsu and Kojima (2002) and Pyne et al. (2003). This effect was related to phosphate buffer concentration and also confirmed that the maintenance of amorphous mannitol is necessary to allow hydrogen bond interactions between mannitol and proteins or other biomolecules and then contribute to stabilize freeze-drying formulations. However, whereas Izutsu et al. (1994) and Pyne et al. (2003) found that mannitol crystalline fraction decreased with an increase on phosphate buffer concentration, we found the opposite dependence. This different behavior could be attributed to the fact that these authors used a ratio phosphate/mannitol 10-fold larger than those used in the present study and/or to the presence of dispersed hydrophobic material in  $\beta$ -carotene samples. In fact, it is interesting to note that even at the low concentrations used in present work, phosphate anions may also act affecting the crystallization patterns through hydrophobic interactions (Gejl-Hansen and Flink, 1977; Elizalde et al., 2002).

The differences on the degree of encapsulation among formulations with different cations could be attributed to the fact that divalent cations may form complexes with hydroxyl group of manitol, and consequently diminish or delay mannitol crystallization. In fact, Angyal (1973) showed that cyclic polyhydroxyl alcohols (epi-inositol) and sugar with hydroxyl groups in axial *cis* position (such as mannitol), formed stable complexes. The differences between cations could be related to the charge/radium ratio and/or coordination numbers (Angyal, 1973).

Regarding the interactions with anionic molecules, Yoshinari et al. (2003) and Izutsu et al. (2004), showed that mannitol hydroxyl groups of C<sub>6</sub> and C<sub>1</sub> (electron donors) form hydrogen bond with the boron central atom (electron acceptor) of sodium tetraborate and boric acid. Therefore, when solid mannitol is produced from aqueous solution in presence of such anions the formation of hydrogen bonds necessary to form a crystalline mannitol network, can be prevented by the mannitol/borate-boric acid or mannitol/divalent cation molecular interactions. Phosphate anions, being strong electron acceptors could interact in the same way with hydroxyl mannitol electron donors at C<sub>1</sub> and C<sub>6</sub> and form a complex, thus inhibiting mannitol crystallization.

Formulations containing divalent cations also showed a better protective effect compared to those with of phosphate buffer alone during freeze-drying of proteins and enzymes (Carpenter et al., 1986, 1987a,b).

The increased  $\beta$ -carotene encapsulation effect of mannitol/glycine formulation (H, Fig. 1) was in accord to previous studies that showed that glycine inhibit mannitol crystallization and that the lyoprotectant effect of mannitol–glycine combinations on an enzyme (lactate dehydrogenase, LDH) was related to the fraction of solutes remaining amorphous during the freeze-drying (Pikal et al., 1991; Pyne et al., 2003). Glycine–mannitol

formulations afforded greater protection at high % RH conditions than the ones with phosphate buffers and divalent cations. However, although glycine inhibited mannitol crystallization, it did not have any effect on  $\beta$ -carotene degradation. The properties of glycine in stabilizing the amorphous characteristics of the materials should be based in different mechanisms than those of ionic compounds. It is possible that glycine forms a physical barrier on the surface of the discontinuous phase. It is thus interesting to note that the mechanism of stabilization of the amorphous phase may play a role in the degradation of encapsulated compounds.

Eq. (1) was adequate to describe the kinetics of the retention of  $\beta$ -carotene in a mannitol matrix containing phosphate buffer 50 mM. That mathematical model had been employed by Levi and Karel (1995) to fit the fractional retention of *n*-propanol entrapped in carbohydrate glasses (of sucrose, and sucrose-*raffinose*) as a function of time, while Elizalde et al. (2002) and Prado et al. (2006) successfully described  $\beta$ -carotene retention encapsulated in trehalose and PVP-40 matrices, respectively, through Eq. (1).

The kinetic parameters for  $\beta$ -carotene degradation ( $k_D$  and  $R_\infty$ ) obtained through Eq. (1) were affected by % RH and by structural properties of the matrix. Serris and Biliaderis (2001) and Selim et al. (2000) found that the first-order rate constants for saffron and beetroot pigments degradation (respectively), encapsulated in polymeric matrices, increased with increasing % RH until a value at which the samples collapsed, and then the rate constants diminished. However, Rodríguez-Huezo et al. (2004) found that a maximum degradation rate of a combination of carotenoids encapsulated in hydrocolloids in spray-dried multiple emulsions occurred at 64% RH; while Prado et al. (2006) found that the rate constant of  $\beta$ -carotene encapsulated in PVP-40 diminished as % RH increased, occurring a change in kinetic behavior at the % RH value at which where the samples collapsed and also in the collapsed samples the kinetic rate constants for  $\beta$ -carotene degradation were notably lower than those corresponding to the gassy state. These different kinetic responses are determined by the mobility of reactants (oxygen diffusion) which is in turn dependent of macrostructure and porosity of the matrix (Selim et al., 2000) and it is thus related to the structural characteristics of the matrices (feasibility to collapse and/or crystallize). Moreau and Rosemberg (1996, 1998) demonstrated that the permeability of wall matrix to oxygen is affected by porosity and this determines the stability of core material. The structural collapse caused the disappearance or the dramatic decrease of micropores through which oxygen can enter or move in the amorphous matrix and through which all diffusion is observed (Moreau and Rosemberg, 1998). Other factors influencing the degradation patterns are the encapsulation method and the matrix composition (crystalline versus polymeric matrix).

Surface color changes in  $\beta$ -carotene encapsulated in polymers such as maltodextrins or PVP followed the same trends as those obtained in the present work for the non-collapsed samples (Desobry et al., 1997; Prado et al., 2006). The surface color changes were significantly affected by the degree of matrix hydration and collapse phenomena: mannitol matrix was visu-

ally perceived as opaque and white in the samples that retained structure and it became translucent in the collapsed samples, allowing to detect the encapsulated pink pigment in the inside. Thus, the obtained  $k_{\text{color}}$  values were not representative of  $\beta$ -carotene retention inside the matrices.

In conclusion, as % RH in the freeze-dried samples increased, degradation rate of  $\beta$ -carotene increased. However, at the point at which the collapse of matrix occurred as a consequence of water plasticization of the solutes, the diffusion of oxygen from the surface to the inside of the matrix possibly diminished and retention increased.

The presence of phosphate salts delayed mannitol crystallization at a highly satisfactory degree during freeze-drying and consequently increased the degree of initial  $\beta$ -carotene encapsulated in the mannitol matrix. This effect was maintained over quite long time during storage of the freeze-dried samples at 25 °C. However, unavoidable local variations in water content during 3 years storage caused the decrease of  $T_g$  values and made the crystallization degree to increase. Divalent cations showed a synergistic effect causing a noticeable increase of initial encapsulation degree compared to mannitol matrix containing only phosphate buffer and also affected the kinetic of  $\beta$ -carotene degradation during storage.

The mechanism of crystallization inhibition likely includes a change in hydrogen bond network or/and change in molecular mobility in the presence of divalent cations and phosphate anions.

The results of this research could be useful to obtain formulations for preserving and stabilizing pharmaceuticals, nutraceuticals and food additives of high cost during freeze-drying and storage.

## Acknowledgements

The authors acknowledge financial support from Universidad de Buenos Aires (Projects EX 274 and EX 182), CONICET (PIP 2734) and ANPCYT-PICT 20545.

## References

- Angyal, S.J., 1973. Complex formation between sugars and metal ions. *Appl. Chem.* 35, 131–146.
- Bendich, A., Olson, J.A., 1989. Biological actions of carotenoids. *FASEE J.* 3, 1927–1932.
- Brazel, C.S., 1999. Microencapsulation offering solutions for the food industry. *Cereal Food World* 44, pp. 338–390, 392–393.
- Burger, A., Henck, J.O., Hetz, S., Rollinger, J.M., Weissnicht, A.A., Stotner, H., 2000. Energy/temperature diagram and compression behaviour of the polymorphs of D-mannitol. *J. Pharm. Sci.* 89, 457–468.
- Carpenter, J.F., Hand, S.C., Crowe, L.M., Crowe, J.H., 1986. Cryoprotection of phosphofructokinase with organic solutes: characterization of enhanced protection 9 in the presence of divalent cations. *Arch. Biochem. Biophys.* 250, 505–512.
- Carpenter, J.F., Crowe, L.M., Crowe, J.H., 1987a. Stabilization of phosphofructokinase with sugars during freeze-drying: characterization of enhanced protection in the presence of divalent cations. *Biochem. Biophys. Acta* 923, 109–115.
- Carpenter, J.F., Martin, B., Crowe, L.M., Crowe, J.H., 1987b. Stabilization of phosphofructokinase during air-drying with sugars and sugars transition metal mixtures. *Cryobiology* 24, 455–464.



- Cavatur, R.K., Vemuri, N.M., Pyne, A., Chrzan, Z., Toledo, Valasquez, D., Suryanarayanan, R., 2002. Crystallization behavior of mannitol in frozen aqueous solutions. *Pharm. Res.* 19, 894–900.
- Chen, B.H., 1992. Studies of the stability of carotenoids in garland chrysanthemum as affected by microwave and conventional heating. *J. Food Prot.* 55, 296–300.
- Constantino, H.R., Andya, J.D., Nguyen, P.E., Dasovich, N., Sweeney, T.D., Shire, S.J., Hsu, C.C., Maa, Y.F., 1998. Effect of mannitol crystallization and aerosol performance of a spray-dried pharmaceutical protein recombinant humanized anti-IgE monoclonal antibody. *J. Pharm. Sci.* 87, 1406–1408.
- Crowe, J.H., Carpenter, J.F., Crowe, L.M., 1998. The role of vitrification in anhydrobiosis. *Annu. Rev. Physiol.* 60, 73–103.
- Delgado Vargas, E., Jiménez, A.R., Paredes-López, O., 2000. Natural pigments. Carotenoids, anthocyanins and betalains—characteristics, biosynthesis, processing and stability. *Crit. Rev. Food Sci. Nutr.* 40, 173–289.
- Desobry, S.A., Netto, F.M., Labuza, T.P., 1997. Comparison of spray-drying, drum drying and freeze-drying for  $\beta$ -carotene encapsulation and preservation. *J. Food Sci.* 62, 1158–1162.
- Elizalde, B.E., Herrera, L., Buera, M.P., 2002. Retention of  $\beta$ -carotene encapsulated in a trehalose matrix as affected by moisture content and sugar crystallization. *J. Food Sci.* 57, 3039–3045.
- Etzel, M.R., Judson King, C., 1980. Retention of volatile components during freeze-drying of substances containing emulsified oils. *J. Food Technol.* 15, 577–588.
- Fakes, M.G., Dali, M.V., Haby, T.A., Morris, K.R., Varia, S.A., Serajuddin, T.M., 2000. Moisture sorption behavior of selected bulking agents used in lyophilized products. *PDA J. Pharm. Sci. Technol.* 54, 144–149.
- Gejl-Hansen, F., Flink, J.M., 1977. Freeze-dried carbohydrate containing oil-in-water emulsions: microstructure and fat distribution. *J. Food Sci.* 42, 1049–1055.
- Giovannucci, E., 1999. Tomatoes, tomato-based products, lycopene and cancer: review of the epidemiological literature. *J. Nat. Cancer Inst.* 91, 317–331.
- Greenspan, L., 1977. Humidity fixed points of binary saturated aqueous solutions. *J. Res. Natl. Bureau Standards* 81A, 89–102.
- Izutsu, K., Yashioka, S., Terao, T., 1993. Decreased protein stabilizing effects of cryoprotectants due to crystallization. *Pharm. Res.* 10, 1232–1237.
- Izutsu, K., Yashioka, S., Terao, T., 1994. Effects of mannitol crystallinity on the stabilization of enzymes during freeze-drying. *Chem. Pharm. Bull.* 42, 5–8.
- Izutsu, K., Kojima, S., 2002. Excipient crystallinity and its protein-structure stabilizing effect during freeze drying. *J. Pharm. Pharmacol.* 54, 1033–1039.
- Izutsu, K., Ocheda, S.O., Aoyagi, N., Kojima, S., 2004. Effects of sodium tetraborate and boric acid on nonisothermal mannitol crystallization in frozen solutions and freeze-dried solids. *Int. J. Pharm.* 273, 85–93.
- Johnson, R.E., Kirchhoff, C.E., Gaud, H.T., 2002. Mannitol–sucrose mixtures—versatile formulations for protein lyophilization. *J. Pharm. Sci.* 91, 914–922.
- Karel, M., Saguy, I., 1991. Effects of water on diffusion in food systems. In: Levine, H., Slade, L. (Eds.), *Water Relationships of Foods*. Plenum Press, New York, pp. 157–173.
- Karel, M., 1991. Physical structure and quality of dehydrated foods. *Drying*, 26–35.
- Kett, V.I., Fitzpatrick, S., Cooper, B., Craig, D.Q., 2003. An investigation into the subambient behaviour of aqueous mannitol solutions using differential scanning calorimetry, cold stage microscopy and X-ray diffractometry. *J. Pharm. Sci.* 92, 1919–1929.
- Kim, A.I., Akers, M.J., Nail, S.L., 1998. The physical state of mannitol after freeze-drying: effects of mannitol concentration, freezing rate and a non-crystallizing cosolute. *J. Pharm. Sci.* 87, 931–935.
- Labrousse, S., Roos, Y., Karel, M., 1992. Collapse and crystallization in amorphous matrices with encapsulated compounds. *Science des Aliments* 12, 757–769.
- Lamikanra, O., 1985. Feasibility of sulphite mediated  $\beta$ -carotene destruction in heterogeneous systems and carrots. *J. Food Process. Preserv.* 9, 209–215.
- Levi, G., Karel, M., 1995. The effect of phase transitions on release of *n*-propanol entrapped in carbohydrate glasses. *J. Food Eng.* 24, 1–13.
- Martini, A., Kune, R.E., Crivelente, M., Artico, R., 1997. Use of subambient differential scanning calorimetry to monitor the freeze-state behaviour of blends of excipients for freeze-drying. *PDA J. Pharm. Sci. Technol.* 51, 62–67.
- Maa, Y.F., Constantino, H.R., Nguyen, P.A., Hsu, C.C., 1997. The effect of operating and formulations variables in the morphology of spray dried protein particles. *Pharm. Dev. Technol.* 2, 213–223.
- Maa, Y.F., Nguyen, P.A., Andya, J.D., Dasovich, N., Sweeney, T.D., Shire, S.J., Hsu, C.C., 1998a. Effect of spray drying and subsequent processing conditions on residual moisture content and physical/biochemical stability of protein inhalation powders. *Pharm. Res.* 15, 768–775.
- Maa, Y.F., Nguyen, P.A., Hsu, C.C., 1998b. Spray drying of air liquid interface sensitive recombinant human growth hormone. *J. Pharm. Sci.* 87, 152–159.
- Mazzobre, M.F., Buera, M.P., 1999. Combined effects of trehalose and cations on the thermal resistance of  $\beta$ -galactosidase in freeze-dried systems. *Biochim. Biophys. Acta* 1473, 337–344.
- Moreau, D.L., Roseberg, M., 1996. Oxidation stability of anhydrous milk fat microencapsulated in whey proteins. *J. Food Sci.* 61, 39–43.
- Moreau, D.L., Roseberg, M., 1998. Porosity of whey-based microcapsules containing anhydrous milk fat measured by gas replacement pycnometry. *J. Food Sci.* 63, 819–823.
- Murakoshi, M., Kato, T., Misawa, N., Narisawa, T., Takasuka, N., Yano, M., 1999. Cancer prevention by carotenoids. *Pure Appl. Chem.* 71, 2273–2278.
- Naesens, W., Tobback, P., 1984. Triglyceride distribution in a low moisture food model system. *J. Food Sci.* 49, pp. 934–938, 947.
- Nail, S.L., Jiang, S., Chongprasert, S., Knopp, S.A., 2002. Fundamentals of freeze-drying. *Pharm. Biotechnol.* 14, 281–360.
- Nishino, H., Tokuda, H., Satomi, Y., Masuda, M., Bu, P., Onozuka, M., Yamaguchi, S., Okuda, Y., Takayasu, J., Tsuruta, J., Okuda, M., Ichilsi, E., Murakoshi, M., Kato, T., Misawa, N., Narisawa, T., Takasuka, N., Yano, M., 1999. Cancer prevention by carotenoids. *Pure Appl. Chem.* 71, 2273–2278.
- Omatete, O.O., Judson King, C., 1978. Volatiles retention during rehumidification of freeze-dried food models. *J. Food Technol.* 13, 265–280.
- Pikal, M.J., Delleman, K.M., Roy, M.I., Riggins, R.M., 1991. The effects of formulation variables on the stability of freeze-dried human growth hormone. *Pharm. Res.* 8, 427–436.
- Prado, S.M., Buera, M.P., Elizalde, B.E., 2006. Structural collapse prevents  $\beta$ -carotene loss in a super-cooled polymeric matrix. *J. Agric. Food Chem.* 54, 79–85.
- Pyne, A., Sarana, R., Suryanarayanan, R., 2002. Crystallization of mannitol below  $T'_g$  during freeze-drying in binary and ternary aqueous systems. *Pharm. Res.* 19, 901–908.
- Pyne, A., Koustov, C.h., Suryanarayanan, R., 2003. Solute crystallization in mannitol–glycine systems. Implications on protein stabilization in freeze-dried formulations. *J. Pharm. Sci.* 92, 2272–2283.
- Qui, Z.H., Xu, A., 1999. Starch-based ingredients for favor encapsulation. *Cereal Food World* 44, 460–465.
- Randolph, T., 1997. Phase separation of excipients during lyophilization: effects on protein stability. *J. Pharm. Sci.* 86, 1198–1203.
- Rodríguez-Huezo, M.E., Pedroza-Islas, R., Prado-Barragán, L.A., Beristain, C.I., Vernon-Carter, E.J., 2004. Microencapsulation by spray-drying of multiple emulsions containing carotenoids. *J. Food Sci.* 69, 7-E351–7-E356.
- Roos, Y.H., Karel, M., 1991. Plasticizing effect of water in thermal behavior and crystallization of amorphous food models. *J. Food Sci.* 56, 38–43.
- Roos, Y.H., 1987. Effect of moisture in the thermal behavior of strawberries studied using differential scanning calorimetry. *J. Food Sci.* 52, 146–149.
- Selim, K., Tsimidou, M., Biliaderis, C.G., 2000. Kinetic studies of saffron carotenoids encapsulated in amorphous polymer matrices. *Food Chem.* 71, 199–206.
- Serris, G.S., Biliaderis, C.G., 2001. Degradation of beetroot pigment encapsulated in polymeric matrices. *J. Sci. Food Agric.* 81, 691–700.
- Shimada, Y., Roos, Y., Karel, M., 1991. Oxidation of methyl linoleate encapsulated in amorphous lactose-based food model. *J. Agric. Food Chem.* 39, 637–641.
- Szpylka, J., DeVries, J.W., 2005. Determination of beta-carotene in supplements and raw materials by reversed-phase high pressure liquid chromatography: collaborative study. *JAOAC Int.* 88, 1279–1291.

- Suzuki, T., Imamura, K., Yamamoto, K., Satoh, T., Okazaki, M., 1997. J. Chem. Eng. Jon. 30, 609–613.
- Tant, M.R., Wilkes, G.L., 1981. An overview of the nonequilibrium behavior of polymers glasses. Polym. Eng. Sci. 21, 874–895.
- Telang, C., Yu, I., Suryanarayanan, R., 2003. Effective inhibition of mannitol crystallization in frozen solutions by sodium chloride. Pharm. Res. 20, 660–667.
- Yoshinari, T., Forbes, R.T., York, P., Karawahisma, Y., 2003. Crystallization of amorphous mannitol is retarded using boric acid. Int. J. Pharm. 258, 109–120.
- Yu, I., Milton, N., Groleau, E.G., Mishra, D.S., Vansickle, R.E., 1999. Existence of a mannitol hydrate during freeze-drying and practical implications. J. Pharm. Sci. 88, 196–198.